



## Design and Simulation Electrothermal Double-Step Structure for Out-of-Plane Actuation

Truong Giang Nguyen<sup>1</sup>, Ngoc Dang Khoa Tran<sup>2</sup>

<sup>1</sup>Faculty of Mechanical Engineering, Industrial University Of Ho Chi Minh City, Ho Chi Minh City, Vietnam, [nguyentruonggiang@iuh.edu.vn](mailto:nguyentruonggiang@iuh.edu.vn)

<sup>2</sup>Faculty of Mechanical Engineering, Industrial University Of Ho Chi Minh City, Ho Chi Minh City, Vietnam, Corresponding author : [tranngocdangkhoa@iuh.edu.vn](mailto:tranngocdangkhoa@iuh.edu.vn)

### ABSTRACT

Out-of-plane actuators have a vital role in the micro-electro-mechanical system (MEMS). Various thermal actuators are applied for the mechanism. The paper proposed the development of a double-stepped beam structure for large out-of-plane displacement output. The structure combines the flexible segments and rigid links. The Joule heating effect drives the device. The performance of this mechanism is the analysis and simulated by Abaqus software. Compared to a single stepped beam design reported in the literature, the proposed double-stepped beam structure can deliver a much larger out-of-plane displacement. Under an applied current of 6 mA, the double stepped beam's maximum deflection is nearly three times higher than that of the single stepped beam structure. The effects of stepped beam parameters are investigated in the design mechanism.

**Key words :** Temperature, displacement, current, stepped beam.

### 1. INTRODUCTION

Microactuators provide the amount of energy for the operation of the micromechanical system. They have many implementations in biomedical fields [1], sensors [2], positioning devices [3], gripper systems [4]. For the linear motions, there are two kinds of movements considered by the researchers and they are in-plane and out-of-plane motion stages. Many researched in-plane motion are reported with many applications [5-8].

Furthermore, out-of-plane microactuators also find applications in optical switches, micromirrors, etc. Many microscale out-of-plane motion mechanisms have been developed. Guo *et al.* [9] introduce an out-of-plane constructed by prestrain-free-dielectric elastomer film with a massive displacement. Micheal and Kwok [10] developed a mechanism for micro- lens device operation based on the piezoelectrical system. An out-of-plane mechanism with two

microbeams and work with electrostatic force has been investigated by Ouakad [11]. Atre [12] presented a bimorph out-of-plane motion mechanism using a two-layer structure where a thin arm is located below a sweeping arm. Bimorph structures have long been studied and used for sensors and actuators because of their sensitivity, fast response time and ease of integration with semiconductor technology. Compared to the stepped beam structure, the bimorph structure adds some complexities to the fabrication process. Moreover, the performance of multi-material microactuators is limited by reduced reliability due to low yield strength and local plastic deformation of their high coefficients of thermal expansion metal layer and delamination at the interface of the two materials caused by substantial thermal shear stress.

Besides the out-of-plane actuator developed based on the electrostatic and electromagnetic, electrothermal actuators also have been applied for many manipulation devices [13]. A simple out-of-plane mechanism is demonstrated by Ogendo *et al.* [14], the structure consists several beams and hinges which have large deflection. Chen *et al.* [15] introduced a single layer thermal actuator move in two directions. Ali *et al.* [16] investigated an out-of-plane electrothermal microactuator based on a single stepped beam. Due to its asymmetric structure, the fabrication process may require more steps. Chen *et al.* [17] demonstrated a step-bridge structure to act as an out-of-plane electrothermal actuator. McCarthy *et al.* [18] designed a long slender single stepped beam that can buckle under thermal loading. The electroplated nickel beams with slight eccentricities offer an out-of-plane motion. Kim *et al.* [19] developed a single stepped beam structure for realizing out-of-plane motion. The height difference from the step features in the beam generates a bending moment from the thermal expansion. Its structure is quite simple for micro-scale fabrication. Simulation is the popular method use to analyze the characteristic of the MEMS devices []. Almost the analysis in thermal actuators implemented the finite element method (FEM) due to the relation between electrical, thermal and mechanical analysis. Li *et al.* [21] investigate an out-of-plane mechanism with the assist of FEM to evaluate the characteristic of the model.

In order to produce larger out-of-plane motion, a double-stepped beam structure is developed in this investigation. The double-stepped beam structure acts like three compliant hinges which provide a rotational degree of freedom to increase the out-of-plane displacement output. An electro-thermo-mechanical finite element model investigates the behavior of the device. The performance of the device is compared with the single stepped beam structure.

**2. DESIGN**

Figure 1(a) is a schematic of the double-stepped beam to convert in-plane motion into out-of-plane motion. A Cartesian coordinate system is also shown in the figure. The structure is similar to two rigid links connected by flexible hinges. As shown in figure 1(b), upon applying an input current through the beam, the beam is loaded by axial compressive force at each end due to thermal expansion. As a result of the bending moment induced by the compressive force, the beam structure experiences an out-of-plane deflection. When the current is relieved, the beam retracts to its original shape, as depicted in figure 1(c).

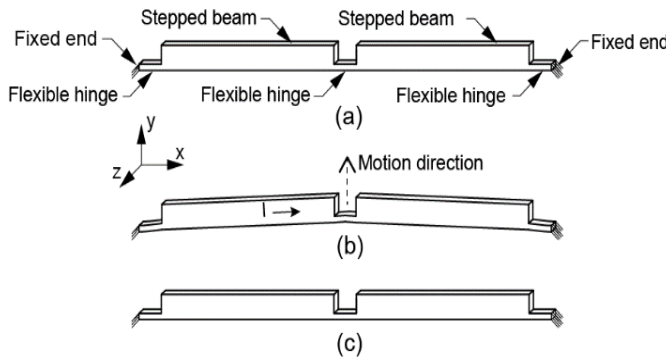


**Figure 1:** Operational principle.

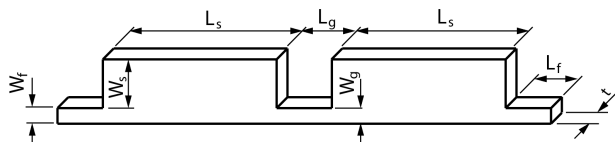


**Figure 2:** Design parameters of the double stepped beam..

Figure 2 illustrates the parameters of the double stepped beam structure. The  $L_s$  and  $W_s$  are the length and the width of the stepped beam.  $L_f$  and  $W_f$  are the dimensions of flexible beam.  $L_g$  and  $W_g$  are the dimensions of the flexible beam between two stepped beam. All the values of the parameters are shown in table 1. The structure is uniform in the thickness,  $t$  is  $5\mu\text{m}$ . At the microscale, heat conduction is dominant over free convection, while radiation is negligible. In this investigation, the convection and radiation effects are neglected in the electrical-thermal step. The element, DC3D8E, is employed in the coupled electrical-thermal analysis to get the beam's temperature distribution. Both ends of the beam are assumed to be linked directly to a heat sink,

which is at room temperature ( $20^\circ\text{C}$ ). A 1 mm gap between the beam and substrate is also assumed to consider the heat conduction between the beam and the substrate. Figure 3 is a cross-sectional view to illustrate the heat transfer path of the beam structure.

**Table 1:** Dimension of double stepped beam

Parameters	Value
$L_f$ ( $\mu\text{m}$ )	20
$L_s$ ( $\mu\text{m}$ )	240
$L_g$ ( $\mu\text{m}$ )	20
$W_f$ ( $\mu\text{m}$ )	5
$W_s$ ( $\mu\text{m}$ )	15
$W_g$ ( $\mu\text{m}$ )	5

In the second step, thermal-mechanical analysis, the ends of the beam are mechanically fixed while all other boundaries are kept free to move. The element, C3D8R, is used for this step. Silicon is selected as the material of the beam. The material is assumed to be linear elastic. The material properties are listed in Table 2.

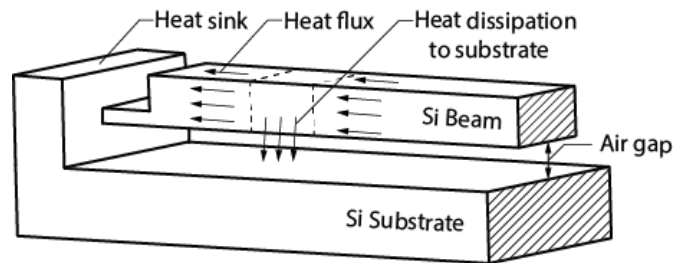


**Figure 3:** The heat transfer path of the beam.

Resistivity and thermal expansion coefficient of silicon are temperature dependent. The resistivity of the material is assumed as [9, 12]

$$\rho = -0.467 \times T + 400 \tag{1}$$

The thermal conductivity of the material is given as

$$\rho = (5 \times 10^{-4}) \times T^2 - 0.4706 \times T + 164.15 \tag{2}$$

where the temperature is in degrees Celsius and the thermal conductivity is in  $\text{W/m}^\circ\text{C}$ . The coefficient of thermal expansion is

$$\alpha = (3 \times 10^{-9}) \times T + 3 \times 10^{-6} \tag{3}$$

where the temperature is in degrees Celsius.

**3. SIMULATION**

The process of simulation of the mechanism is proposed in figure 4. In order to analyze the deformation of the beam under current loading. Three-dimensional finite element analyses are employed. The electro-thermo-mechanical

analysis is carried out in two steps. The first step is the electrical-thermal analysis, investigate the transfer of the current into temperature. The mesh model put in the Abaqus program and boundary conditions are applied to the model. Current applied to the model at the fixed end of beams. Abaqus analyzes the temperature of the structure when the current increase. After analysis, the temperature contributes to the beam is adopted. The next step of thermal-mechanical analysis, the deflection of the beam is analyzed. The initial temperature of the whole device is assumed at 20oC in the electrical-thermal step. The temperature is applied to the structure with the same mesh model in step one and the boundary conditions are either. The deflection analysis obtains the movement of the beam. The middle point is investigated to observe the deflection process.

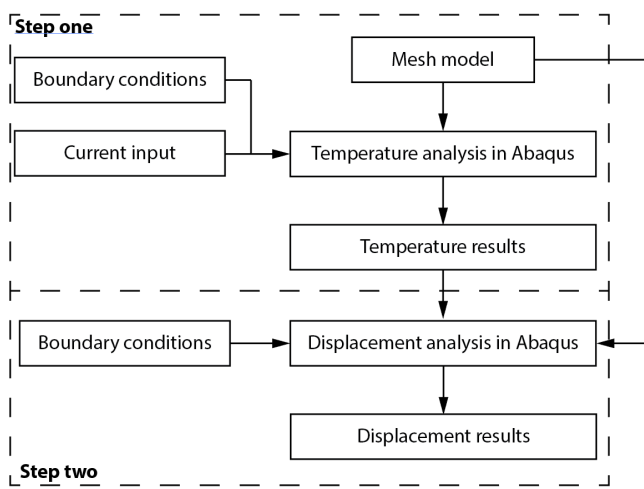


**Figure 4:** Process of the simulation of double step model.

Figure 5(a) shows a mesh for a finite element model. The finite element model has 6300 8-node elements. A mesh convergence study is performed to obtain accurate solutions of displacement solutions. A close-up view of the mesh near the fixed end of the beam is also shown in the figure. Fig. 4(b) shows a deformed mesh when a current is applied to the ends of the beam.

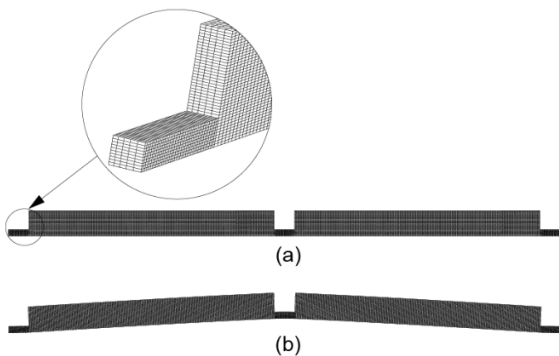


**Figure 5:** (a) Undeformed mesh and (b) deformed mesh of the finite element model.

**4. RESULT AND DISCUSSION**

Figure 6 shows the temperature contour along the beam at a current of 8 mA and celsius units of degree. Due to the heat sink assumption attached to both ends, the temperature is symmetric with respect to the middle plane. The temperature increases rapidly at a flexible hinge close fixed end, the ratio is ten times. In the stepped beam, the heat develops slowly. In the middle of the beam, the highest temperature is obtained, around 600 degrees. The Mises stress contours are depicted in Figure 7. The largest stress, 0.78GPa, is much smaller than the yield strength of typical silicon material (7GPa).

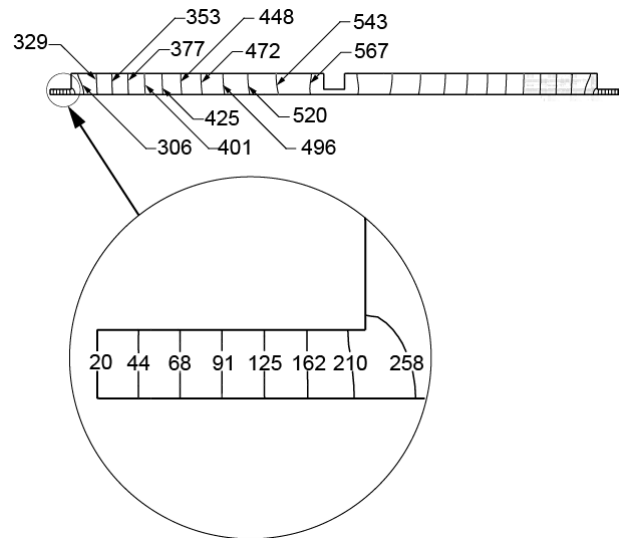


**Figure 6:** Temperature contours (°C) in the beam under a current of 8 mA

Figure 8 shows steady-state temperature distributions along the beam under different currents passing through. The temperature rise is symmetric and proportional to the current. The temperature profile is similar to parabolic curve. The closer to the ends the location is, the lower temperature is observed. This is due to heat conduction to the heat sink. As seen in this figure, the highest temperature is around 75°C at a current of 2 mA and it is nearly 590 °C for the case of 8 mA.

The deflection at the center of the beam corresponding to the input current is plotted in figure 9. The maximum deflection increases gradually with the input current from 1 to 3.5 mA. However, this increase becomes significant at higher input currents ranging from 3.5 to 8 mA. At a current of 8 mA, the maximum deflection is found to be 12.9 mm, with 5900C of the highest temperature in the beam. The maximum deflection of a single stepped beam as a function of the input current is also shown in figure 8. It is obvious that the proposed double-stepped beam structure has a much larger out-of-plane for the current ranging from 3.5 to 8 mA. Especially, the maximum displacement of the double stepped beam structure is about 1.7, 2.9 and 2.6 times greater than

that of the single stepped beam structure with input currents of 4, 6 and 8 mA, respectively.

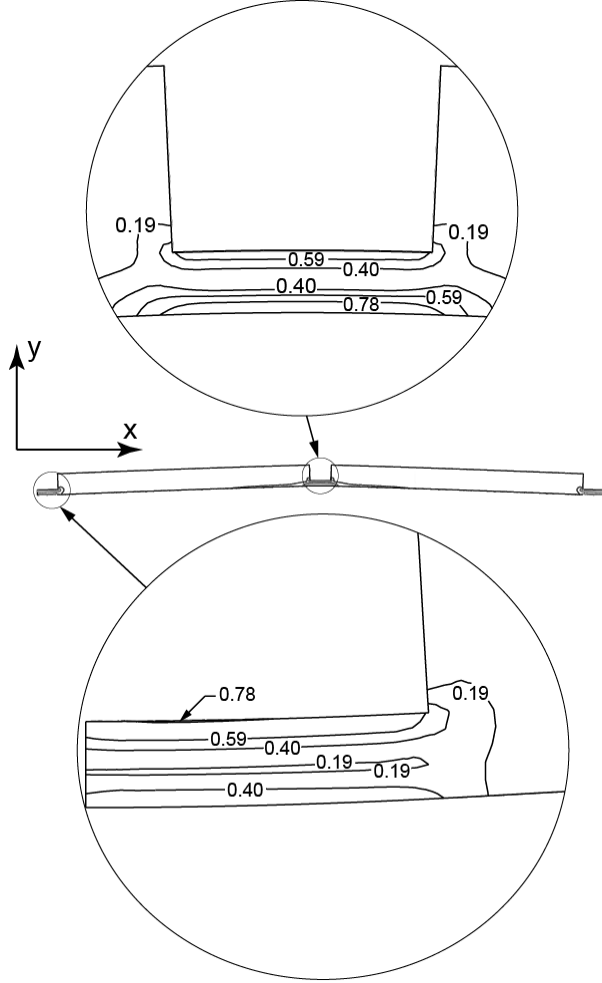


**Figure 7:** Contours of the Mises stress (GPa) in the beam under a current of 8 mA.

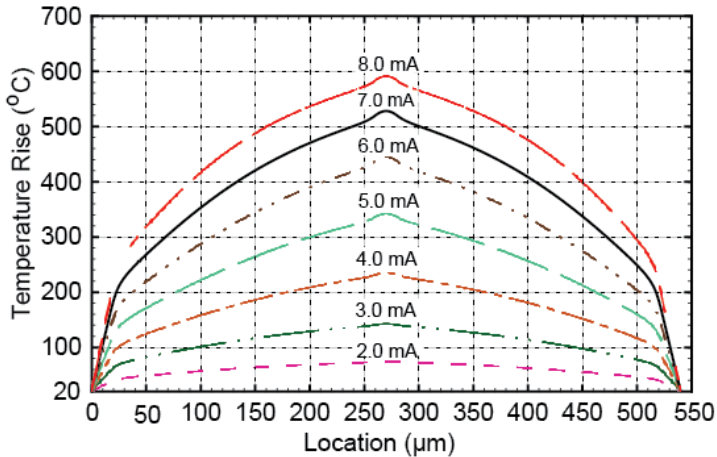


**Figure 8:** Steady state temperature distributions along the beam under different currents passing through.

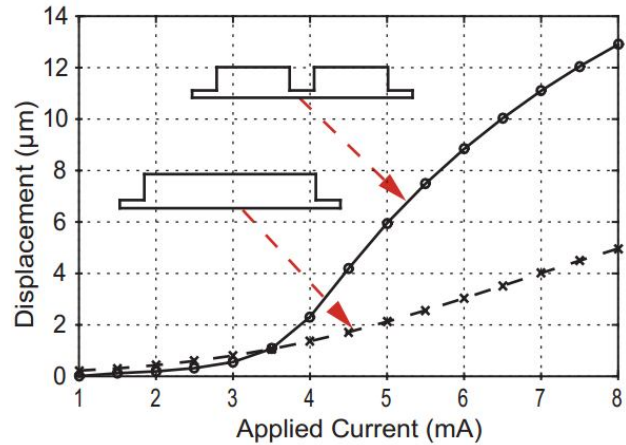


**Figure 9:** Maximum deflection as a function of the input current.

The effects of the step beam are investigated. All the parameters are the same with table 1,  $L_s$  and  $L_g$  are modified to analyze the properties. In order to maintain the total length of the mechanism, when  $L_s$  decrease,  $L_g$  is increased. The result is shown in table 2 with maximum displacement increase. The displacement increase proportional to  $L_g$ . However, the temperature also increases cause the stress of the beam increases.

**Table 2:** Parameters of step beam

$L_s$ ( $\mu\text{m}$ )	$L_g$ ( $\mu\text{m}$ )	Maximum displacement ( $\mu\text{m}$ )
240	20	13.3
230	22	15.2
220	24	18.5
210	26	22.5
200	28	25.7

**5. CONCLUSION**

A new double-stepped beam structure for large out-of-plane motion is proposed. Its excellent performance is validated by finite element analyses. The maximum deflection of the beam structure reaches  $12.9 \mu\text{m}$  under an input current of 8mA, while the temperature rises to  $690^\circ\text{C}$  and the Mises stress value is still far less than the yield strength of typical silicon material base on the finite element analyses. The maximum out-of-plane deflection of the beam structure is 2.9 times higher than that of a single stepped beam structure. The stepped beam parameters investigation indicates that this beam's small length gives the large deflection and massive stress. The double-step structure has the potential to design the MEMS device, which requires long distance movement in linear motion.

## REFERENCES

1. A. Rezk, J. Friend and L. Yeo. **3-Actuation mechanism for microfluidic biomedical devices**, *Microfluidic Devices for Biomedical Applications*, pp.100-138, 2013.
2. S. Lu, D. Chen, R. Hao, S. Luo and M. Wang. **Design, fabrication and characterization of soft sensors through EGaIn for soft pneumatic actuators**, *Measurement*, vol. 164, 2020.
3. H. Wang and X. Zhang. **Input coupling analysis and optimal design of a 3-DOF compliant micro-positioning stage**, *Mechanism and Machine Theory*, vol. 43, issue 4, pp. 400-410, 2008.
4. R. Hugo, W. Wang, D. R. Kim and S. H. Ann. **Curved shape memory alloy-based soft actuators and application to soft gripper**, *Composite Structures*, vol. 176, pp. 398-406, 2017.
5. Y. Lua, Q. Shao, M. Amabili, H. Yue and H. Guo. **Nonlinear vibration control effect of membrane structure with in-plane PVDF actuators: A parametric study**, *International Journal of Non-Linear Mechanics*, vol. 122, 2020.
6. O. Ergeneman, P. Eberle, M. Suter, G. Chatzipirpiridis, K. M. Sivaraman, S. Pané, C. Hierold and B. J. Nelson. **An in-plane cobalt-nickel microresonator sensor with magnetic actuation and readout**, *Sensors and Actuators A*, vol. 188, pp. 120-126, 2012.
7. Y. Eun, H. Na, J. Choi, J. Lee and J. Kim. **Angular vertical comb actuators assembled on-chip using in-plane electrothermal actuator and latching mechanism**, *Sensors and Actuators A*, vol. 165, pp. 120-126, 2012.
8. K. Jia, T. Lu and T. Wang. **Deformation study of an in-plane oscillating dielectric elastomer actuator having complex modes**, *Journal of Sound and Vibration*, vol. 463, 2019.
9. D. Guo, Y. Han, Y. Ding, S. Fang and W. Tan. **Prestrain-free electrostrictive film sandwiched by asymmetric electrodes for out-of-plane actuation**, *Chemical Engineering Journal*, vol. 352, pp. 876-885, 2018.
10. A. Micheal and C. Y. Kwok. **Piezoelectrically driven micro-lens out-of-plane actuation**, *Procedia Engineering*, vol. 25, pp. 697-700, 2011.
11. H. M. Ouakad. **Static response and natural frequencies of microbeams actuated by out-of-plane electrostatic fringing-fields**, *International Journal of Non-Linear Mechanics*, vol. 63, 2014.
12. A. Atre. **Analysis of Out-of-Plane Thermal Microactuators**, *Journal of Micromechanics and Microengineering*, Vol.16, pp. 94-100, 2011.
13. S. Alsheri. **Cooling Microprocessors with Commercial Thermoelectric Module Powered by Pulsed Current**, *International Journal of Advanced Trends in Computer Science and Engineering*, vol. 9, no. 4, 2020.
14. K. Ogando, N. L. Forgia, J.J. Zárate and H. Pastoriza. **Design and characterization of a fully compliant out-of-plane thermal actuator**, *Sensors and Actuators A: Physical*, vol. 183, pp. 95-100, 2012.
15. W. Chen, C. Chu, J. Hsieh and W. Fang. **A reliable single-layer out-of-plane micromachined thermal actuator**, *Sensor and Actuators A*, vol. 103, 2003.
16. M. McCarthy, N. Tiliakos, V. Modi, L. G. Frechette. **Thermal buckling of eccentric microfabricated nickel beams as temperature regulated nonlinear actuators for flow control**, *Sensors and Actuators A*, vol. 134, pp. 37-46, 2007.
17. N. S. Ali, M. N. Patricia and K. Amir. **Electrothermomechanical modeling of out-of-plane deformation in single-stepped beams actuated by resistive heating**, *Micromechanics and Microengineering*, vol. 25, 2015.
18. W. C. Chen, P. I. Yeh, C. F. Hu and W. Fang. **Design and Characterization of Single-Layer Step-Bridge Structure for Out-of-Plane Thermal Actuator**, *Journal of Microelectromechanical Systems*, Vol. 17, pp. 70-77, 2008.
19. Y. S. Kim, N. G. Dagalakis and S. Gupta. **Creating Large Out-of-Plane Displacement Electrothermal Motion Stage by Incorporating Beams with step features**, *Journal of Micromechanics and Microengineering*, Vol.23, 055008, 2013.
20. N. D. K. Tran, T. G. Nguyen and T. L. Tran, **Optimal design the compliant bistable mechanism based on NSGA-II**, *International Journal of Advanced Trends in Computer Science and Engineering*, vol. 9, no. 4, 2020.
21. R. Li, Q. Huang and W. Li. **A nodal analysis model for the out-of-plane beamshape electrothermal actuator**, *Microsystem Technologies*, vol. 15, pp. 217-225, 2009.